Journal of Power Sources 230 (2013) 267–270

Contents lists available at SciVerse ScienceDirect

Journal of Power Sources

journal homepage: www.elsevier.com/locate/jpowsour

Short communication

Improving rate performance of $LiMnPO_4$ based material by forming electron-conducting iron phosphides

Shan Liu [a,b,c], Haisheng Fang [a,b,c,*], Bin Yang [a,b,c], Yaochun Yao [a,b,c], Wenhui Ma [a,b,c], Yongnian Dai [a,b,c]

[a] National Engineering Laboratory for Vacuum Metallurgy, Kunming University of Science and Technology, Kunming 650093, Yunnan, China
[b] Faculty of Metallurgical and Energy Engineering, Kunming University of Science and Technology, Kunming 650093, China
[c] Key Laboratory of Nonferrous Metals Vacuum Metallurgy of Yunnan Province, Kunming University of Science and Technology, Kunming 650093, China

HIGHLIGHTS

- Olivine $LiMnPO_4$ based cathode material is synthesized via the controlled nonstoichiometry.
- Electronically conductive phosphides are created on the surface of the $LiMn_{0.8}Fe_{0.19}Mg_{0.01}PO_4$.
- The nonstoichiometric sample shows increased electronic conductivity and rate capability.

ARTICLE INFO

Article history:
Received 9 July 2012
Received in revised form
19 October 2012
Accepted 13 December 2012
Available online 27 December 2012

Keywords:
Lithium ion batteries
Cathode materials
Lithium manganese phosphate
Surface chemistry

ABSTRACT

In the present work, olivine $LiMnPO_4$ based cathode material is synthesized from a nonstoichiometric mixture of starting materials (the chemical composition can be denoted as $LiMn_{0.8}Fe_{0.19+2x}Mg_{0.01}P_{1+x}O_4$, $x = 0.033$) and characterized by X-ray diffraction (XRD), magnetic measurement, scanning electron microscopy (SEM) and electrochemical test. The results show that electronically conductive iron phosphides are created on the surface of $LiMn_{0.8}Fe_{0.19}Mg_{0.01}PO_4$ via the controlled nonstoichiometry and can effectively increase electronic conductivity and rate capability of the obtained material.

1. Introduction

To meet the requirement of lithium ion batteries for new applications such as in electric vehicles, developing advanced cathode materials is highly demanded. As a promising cathode material for lithium ion batteries, olivine $LiMnPO_4$ has recently received increasing attention owing to its high redox potential (4.1 V versus Li/Li^+), low cost and good safety. However, the inherently low ionic and electronic conductivities of $LiMnPO_4$ seriously limit Li^+ insertion/extraction and electron transport in this material [1–3], making it challenging to achieve high rate capability. Strategies to overcome these limitations have focused on surface modification [4–9], particle size reduction [10–12] and cation substitution [13–19], but it is noted that the rate capability of $LiMnPO_4$ could not be significantly increased by cation substitution or particle size reduction without carbon coating [20]. Considering the well-known role of carbon coating, the electron transport at the surface of $LiMnPO_4$ should also be accelerated by creating other electronically conductive phases. In fact, iron phosphides formation via carbothermal reduction has been found to be very effective for increasing electronic conductivity and rate performance of $LiFePO_4$ [21–23], and the improvement does not sacrifice energy density of the material because of the high density of iron phosphides. However, such strategy has not yet been applied for $LiMnPO_4$ probably due to the high reduction temperature (>1000 °C) for producing manganese phosphides [24].

More recently, we have reported that Mn-site Fe&Mg co-substitution could greatly improve the rate performance of $LiMnPO_4$ [25–27]. Based on our previous work on Fe&Mg co-substituted $LiMnPO_4$, herein we report a nonstoichiometry strategy to create active material and electron-conducting iron phosphides simultaneously from a nonstoichiometric mixture of

* Corresponding author. Faculty of Metallurgical and Energy Engineering, Kunming University of Science and Technology, 253 Xuefu Road, Kunming 650093, Yunnan, China. Tel./fax: +86 871 65107208.
E-mail address: hsfang1981@yahoo.com.cn (H. Fang).

0378-7753/$ – see front matter © 2012 Elsevier B.V. All rights reserved.
http://dx.doi.org/10.1016/j.jpowsour.2012.12.080

starting materials (the chemical composition can be denoted as $LiMn_{0.8}Fe_{0.19+2x}Mg_{0.01}P_{1+x}O_4$, $x = 0.033$). The material derived from the nonstoichiometric mixture showed increased electronic conductivity, enhanced rate performance and excellent cycling stability.

2. Experimental

Based on the nominal chemical composition of $LiMn_{0.8}Fe_{0.256}Mg_{0.01}P_{1.033}O_4$, appropriate amounts of LiH_2PO_4, $MnC_4H_6O_4\cdot 4H_2O$, $H_2C_2O_4\cdot 2H_2O$, $FeC_2O_4\cdot 2H_2O$, $MgC_4H_6O_4\cdot 4H_2O$, $NH_4H_2PO_4$ and sucrose were fully ball-milled for 6 h, and then heated (heating rate: 2 °C min^{-1}) at 800 °C for 10 h under an Ar atmosphere. The mole ratio of the excess $FeC_2O_4\cdot 2H_2O$ and $NH_4H_2PO_4$ was controlled to be 2:1. The obtained material was called nonstoichiometric sample. For comparison, stoichiometric sample, $LiMn_{0.8}Fe_{0.19}Mg_{0.01}PO_4$/C, was also synthesized via the same route. In the final product, the carbon content of the stoichiometric and nonstoichiometric samples was 12.7 wt.% and 11.4 wt.%, respectively.

The crystalline phase of the obtained samples was identified by X-ray diffraction (XRD) on apparatus (D/MaX-3B, Rigaku) using Cu K_α radiation, and the lattice parameters were estimated by refining the XRD patterns using Rietica. Materials morphology and particle size were observed by scanning electron microscopy (SEM, XL30, Philips). The M–H curves were obtained on a Physical Property Measurement System (PPMS-9T) at 200 and 300 K. The electronic conductivity was measured using the Four-Probe technique on a 4-point Probes Resistivity Measurement System (RTS-8, Four Probes Tech). Before the conductivity measurement, powders of the two samples were manually pelletized under the pressure of 20 MP using a disk-shaped mould.

Electrochemical properties of the samples were assessed using CR2025 coin-type cells. The cathode was made by mixing active material, super P and polyvinylidene fluoride (PVDF) in a weight ratio of 8:1:1 and stirred to slurry. Then the slurries were coated on aluminium foil by a doctor blade coater. The typical loading of the cathode with a diameter of 1.3 cm was about 2.3 mg active materials. The electrolyte was 1 M $LiPF_6$ in EC/DMC (1/1) solution. All cells were assembled in an argon-filled glove box with lithium metal as the anode. Charge–discharge testing was performed between 2.0 and 4.5 V. Electrochemical impedance spectroscopy (EIS) was carried out in a frequency range from 0.1 Hz to 100 kHz with an AC signal of 5 mV. All electrochemical tests were conducted at 30 °C.

3. Results and discussion

Fig. 1a and b shows XRD patterns of the stoichiometric and non-stoichiometric samples. No apparent difference is observed between the patterns of the two samples, and XRD refinement reveals that the two samples have very similar lattice parameters ($a = 6.0865$ Å, $b = 10.4307$ Å, and $c = 4.7348$ Å for the stoichiometric sample; $a = 6.0824$ Å, $b = 10.4256$ Å, and $c = 4.7332$ Å for the nonstoichiometric sample), which means that the main phase in the nonstoichiometric sample is much close to stoichiometric $LiMn_{0.8}Fe_{0.19}Mg_{0.01}PO_4$ and most of the extra iron and phosphorus do not enter into the lattice of $LiMn_{0.8}Fe_{0.19}Mg_{0.01}PO_4$. On this condition, secondary phases derived from extra iron and phosphorus should be present in the nonstoichiometric sample, but

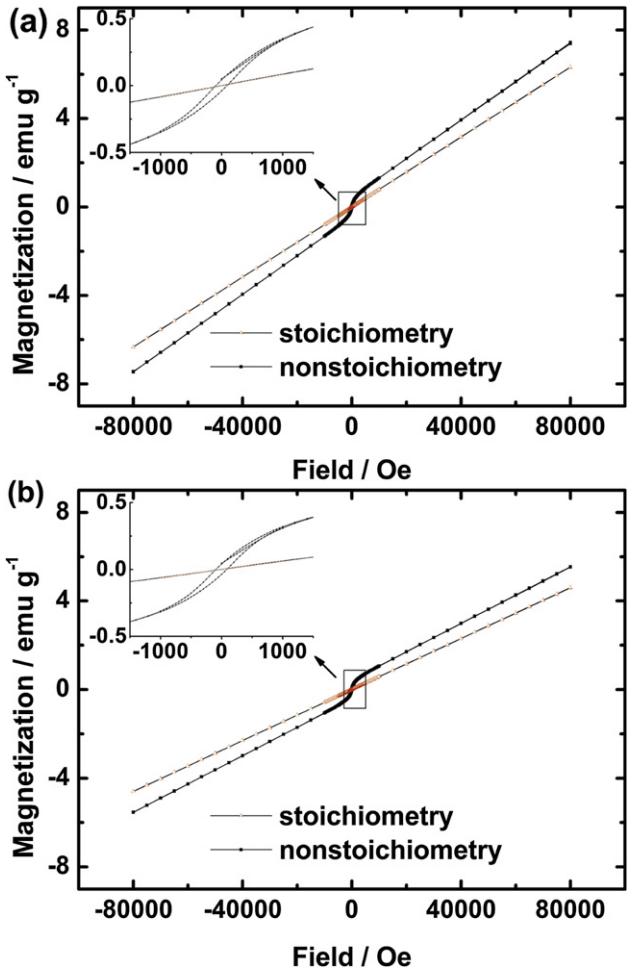

Fig. 2. Magnetization of the stoichiometric and nonstoichiometric samples as a function of the applied field at two different temperatures: (a) 200 K, (b) 300 K.

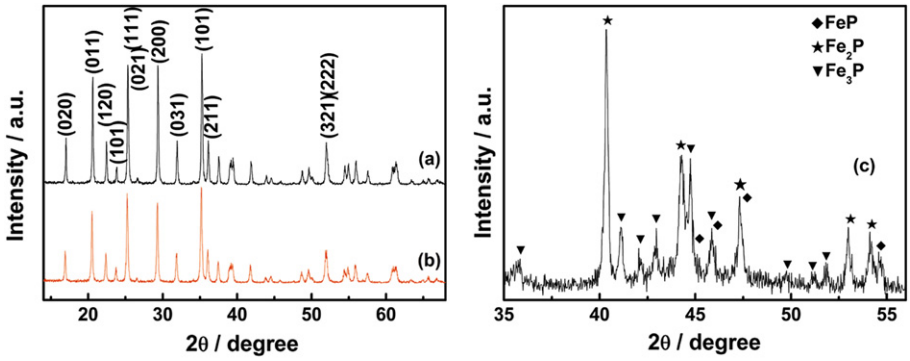

Fig. 1. XRD patterns of (a) the stoichiometric sample, (b) the nonstoichiometric sample, and (c) the product from heating the mixture of $FeC_2O_4\cdot 2H_2O$, $NH_4H_2PO_4$ and sucrose at 800 °C under an Ar atmosphere.

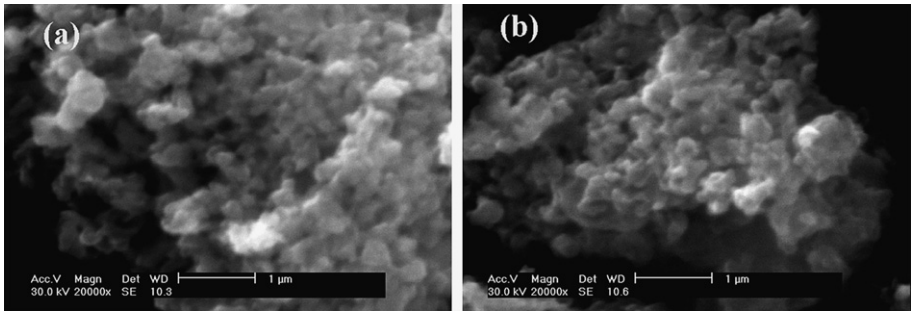

Fig. 3. SEM images of (a) the stoichiometric sample and (b) nonstoichiometric sample.

these phases were not detected by XRD probably due to the small amount and/or the poor crystallized nature. According to available literature [21–24], the present preparation condition should result in the reduction of extra $FeC_2O_4 \cdot 2H_2O$ and $NH_4H_2PO_4$ to electronically conductive iron phosphides. Indeed, independent experiment demonstrated that iron phosphides including FeP, Fe_2P and Fe_3P have been readily generated by heating the mixture of $FeC_2O_4 \cdot 2H_2O$, $NH_4H_2PO_4$ and sucrose at 800 °C under the same condition (Fig. 1c). Moreover, magnetic measurement also supports the formation of iron phosphides in the nonstoichiometric sample. As shown in Fig. 2, different magnetic properties are observed between the stoichiometric and nonstoichiometric samples despite

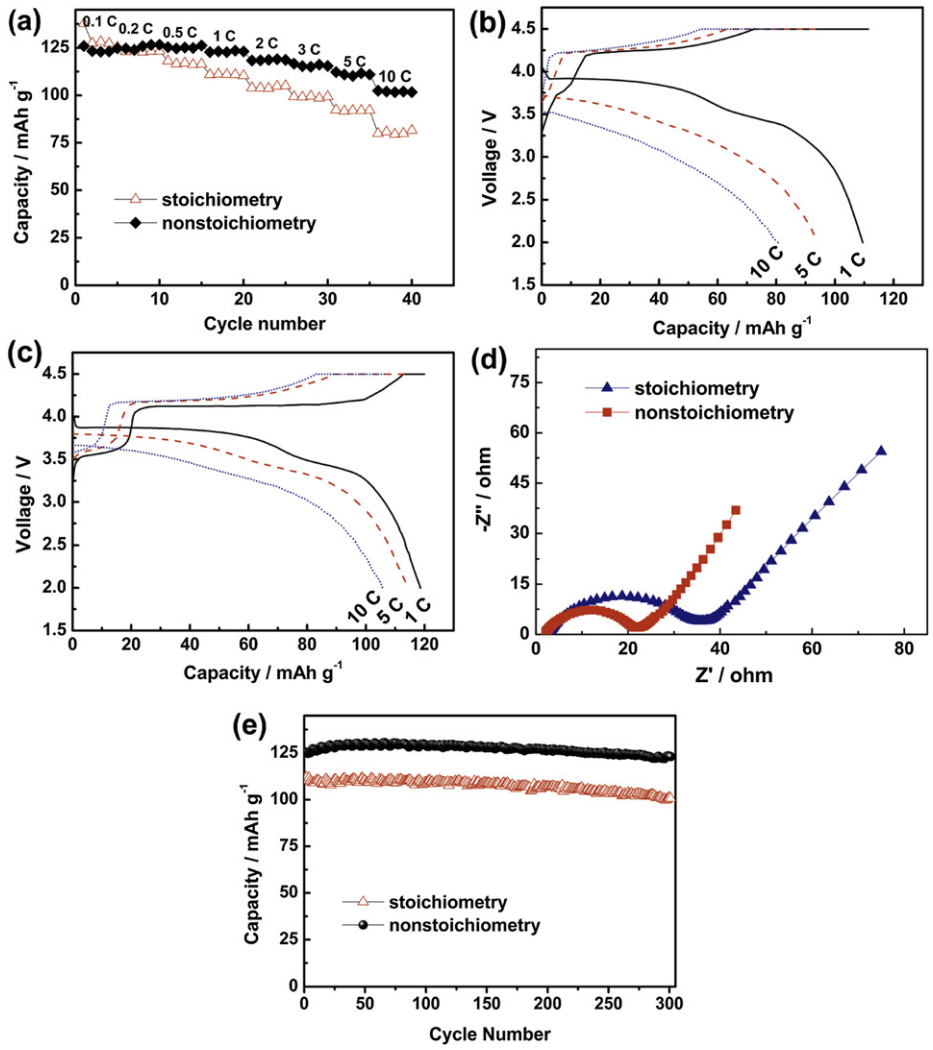

Fig. 4. (a) Rate performance of the stoichiometric and nonstoichiometric samples. Cells were charged at 0.1 C to 4.5 V, held at 4.5 V until the current decreased to 0.01 C and then discharged at various rates to 2.0 V (b) and (c) Typical charge/discharge curves of the stoichiometric and nonstoichiometric samples, respectively. Cells were charged at 1 C to 4.5 V, held at 4.5 V until the current decreased to 0.01 C and then discharged at various rates to 2.0 V (d) EIS plot of the stoichiometric and nonstoichiometric samples recorded at the fully discharged state after the first round rate test. (e) Cycling performance of the stoichiometric and nonstoichiometric samples. Cells were charged at 1 C, held at 4.5 V until the current decreased to 0.01 C and then discharged at 1 C to 2.0 V.

their similar XRD patterns. The magnetization of the stoichiometric sample is linear in the range of the applied magnetic field at the temperatures of 200 and 300 K, which is consistent with the intrinsically antiferromagnetic property of $LiMn_{0.8}Fe_{0.19}Mg_{0.01}PO_4$. However, a small hysteresis loop is observed on the magnetization of the nonstoichiometric sample, which is associated with the presence of ferromagnetic Fe_2P and Fe_3P [21]. Owing to the formation of these electron-conducting iron phosphides, the electronic conductivity of the nonstoichiometric sample has been raised up to 1.41 S cm^{-1} which is over three times that of the stoichiometric one (4.48×10^{-1} S cm^{-1}).

Fig. 3 shows SEM images of the stoichiometric and nonstoichiometric samples. It is seen that the two samples exhibit similar morphology and particle size. The primary particles are around 200–400 nm and agglomerate into micron particles, which give a tap density of 1.1 g cm^{-3} for both samples. From the above results, it is concluded that the controlled nonstoichiometry strategy can create more electronically conductive phases on the surface of $LiMn_{0.8}Fe_{0.19}Mg_{0.01}PO_4$ without affecting the morphology and particle size.

Fig. 4a compares the rate capability of the stoichiometric and nonstoichiometric samples. Cells were charged at 0.1 C (1 C is equal to 150 mA g^{-1}) to 4.5 V, held at 4.5 V until the current decreased to 0.01 C, and then discharged at various rates to 2.0 V. Although both samples show excellent rate performance, the nonstoichiometric sample apparently delivers higher capacities at high rates. The reversible capacity of the nonstoichiometric sample can reach 123 mAh g^{-1} at 1 C, 116 mAh g^{-1} at 3 C, 111 mAh g^{-1} at 5 C and 102 mAh g^{-1} at 10 C. More notably, when the charge rate was increased to 1 C after the former rate test, the discharge capacities at high rates were still retained for both samples. Typical charge/discharge curves at various rates are shown in Fig. 4b and c. Clearly, not only higher discharge capacities but also smaller polarization between charge and discharge curves is observed for the nonstoichiometric sample. Fig. 4d presents EIS plot of the two samples recorded at the fully discharged state after the first round rate test. A much smaller semicircle is observed for the nonstoichiometric sample, indicating the accelerated electron transport over the surface of the active material due to the formation of electron-conducting iron phosphides. These results demonstrate that creating electronically conductive phosphides via our controlled nonstoichiometry can speed up electron transport over the surface and enhance the rate performance of $LiMn_{0.8}Fe_{0.19}Mg_{0.01}PO_4$. In addition, we should point out that the rate and capacity were calculated without deducting the inactive phases (residual carbon and/or phosphides) from the prepared composite in the present work. Even so, the capacities obtained at high rates for the nonstoichiometric sample are still higher than those reported in most available literature [8,12,16,28,29]. More significantly, such a high rate capability is achieved with a tap density of 1.1 g cm^{-3} for the nonstoichiometric sample. Fig. 4e shows cyclability of the stoichiometric and nonstoichiometric samples. Cells were charged at 1 C, held at 4.5 V until the current decreased to 0.01 C and then discharged at 1 C to 2.0 V. The nonstoichiometric sample shows excellent capacity retention upon cycling, and has a higher reversible capacity as compared to the stoichiometric one. Even after 300 cycles, over 98% of the initial capacity was observed for the nonstoichiometric sample.

4. Conclusions

Electron-conducting iron phosphides were created on the surface of $LiMn_{0.8}Fe_{0.19}Mg_{0.01}PO_4$ via our controlled nonstoichiometry. These phases coupled with the residual carbon formed a more effective conductive network for electron transport over the surface of the active material, which led to enhanced rate performance of the $LiMn_{0.8}Fe_{0.19}Mg_{0.01}PO_4$. Moreover, the nonstoichiometric sample also had excellent cycling stability.

Acknowledgements

This work was supported by the Specialized Research Fund for the Doctoral Program of Higher Education (No. 20125314120004) and the Jinchuan Pre-Research Foundation (No. Jinchuan201112).

References

[1] A.K. Padhi, K.S. Nanjundaswamy, J.B. Goodenough, J. Electrochem. Soc. 144 (1997) 1188–1194.
[2] M. Yonemura, A. Yamada, Y. Takei, N. Sonoyama, R. Kanno, J. Electrochem. Soc. 151 (2004) A1352–A1356.
[3] C. Delacourt, L. Laffont, R. Bouchet, C. Wurm, J.B. Leriche, M. Morcrette, J.M. Tarascon, C. Masquelier, J. Electrochem. Soc. 152 (2005) A913–A921.
[4] G. Li, H. Azuma, M. Tohda, Electrochem. Solid State Lett. 5 (2002) A135–A137.
[5] C. Masquelier, C. Delacourt, P. Poizot, M. Morcrette, J.M. Tarascon, Chem. Mater. 16 (2004) 93–99.
[6] Z. Bakenov, I. Taniguchi, J. Power Sources 195 (2010) 7445–7451.
[7] B. Kang, G. Ceder, J. Electrochem. Soc. 157 (2010) A808–A818.
[8] S.M. Oh, S.W. Oh, C.S. Yoon, B. Scrosati, K. Amine, Y.K. Sun, Adv. Funct. Mater. 20 (2010) 3260–3265.
[9] H. Wang, Y. Yang, Y. Liang, L.F. Cui, H. Sanchez Casalongue, Y. Li, G. Hong, Y. Cui, H. Dai, Angew. Chem. Int. Ed. 50 (2011) 7364–7368.
[10] T. Drezen, N.H. Kwon, P. Bowen, I. Teerlinck, M. Isono, I. Exnar, J. Power Sources 174 (2007) 949–953.
[11] D. Wang, H. Buqa, M. Crouzet, G. Deghenghi, T. Drezen, I. Exnar, N.H. Kwon, J.H. Miners, L. Poletto, M. Grätzel, J. Power Sources 189 (2009) 624–628.
[12] D. Choi, D. Wang, I.T. Bae, J. Xiao, Z. Nie, W. Wang, V.V. Viswanathan, Y.J. Lee, J.G. Zhang, G.L. Graff, Z. Yang, J. Liu, Nano Lett. 10 (2010) 2799–2805.
[13] G. Chen, J.D. Wilcox, T.J. Richardson, Electrochem. Solid State Lett. 11 (2008) A190–A194.
[14] S.K. Martha, J. Grinblat, O. Haik, E. Zinigrad, T. Drezen, J.H. Miners, I. Exnar, A. Kay, B. Markovsky, D. Aurbach, Angew. Chem. Int. Ed. 48 (2009) 8559–8563.
[15] T. Shiratsuchi, S. Okada, T. Doi, J.I. Yamaki, Electrochim. Acta 54 (2009) 3145–3151.
[16] J. Kim, D.H. Seo, S.W. Kim, Y.U. Park, K. Kang, Chem. Commun. 46 (2010) 1305–1307.
[17] J.W. Lee, M.S. Park, B. Anass, J.H. Park, M.S. Paik, S.G. Doo, Electrochim. Acta 55 (2010) 4162–4169.
[18] D. Wang, C. Ouyang, T. Drezen, I. Exnar, A. Kay, N.H. Kwon, P. Gouerec, J.H. Miners, M. Wang, M. Grätzel, J. Electrochem. Soc. 157 (2010) A225–A229.
[19] G. Yang, H. Ni, H. Liu, P. Gao, H. Ji, S. Roy, J. Pinto, X. Jiang, J. Power Sources 196 (2011) 4747–4755.
[20] T. Doi, S. Yatomi, T. Kida, S. Okada, J.I. Yamaki, Cryst. Growth Des. 9 (2009) 4990–4992.
[21] P.S. Herle, B. Ellis, N. Coombs, L.F. Nazar, Nat. Mater. 3 (2004) 147–152.
[22] Y.H. Rho, L.F. Nazar, L. Perry, D. Ryan, J. Electrochem. Soc. 154 (2007) A283–A289.
[23] Y. Yin, M. Gao, H. Pan, L. Shen, X. Ye, Y. Liu, P.S. Fedkiw, X. Zhang, J. Power Sources 199 (2012) 256–262.
[24] B. Ellis, P. Subramanya Herle, Y.H. Rho, L.F. Nazar, R. Dunlap, L.K. Perry, D.H. Ryan, Faraday Discuss. 134 (2007) 119–141.
[25] C. Hu, H. Yi, H. Fang, B. Yang, Y. Yao, W. Ma, Y. Dai, Electrochem. Commun. 12 (2010) 1784–1787.
[26] H. Yi, C. Hu, H. Fang, B. Yang, Y. Yao, W. Ma, Y. Dai, Electrochim. Acta 56 (2011) 4052–4057.
[27] H. Fang, E. Dai, B. Yang, Y. Yao, W. Ma, J. Power Sources 204 (2012) 193–196.
[28] Y.K. Sun, S.M. Oh, H.K. Park, B. Scrosati, Adv. Mater. 23 (2011) 5050–5054.
[29] S.M. Oh, S.T. Myung, J.B. Park, B. Scrosati, K. Amine, Y.K. Sun, Angew. Chem. Int. Ed. 51 (2012) 1853–1856.